[Research Paper] 대한금속 · 재료학회지 (*Korean J. Met. Mater.*), Vol. 61, No. 8 (2023) pp.602-607
DOI: 10.3365/KJMM.2023.61.8.602

Transition Metal Dichalcogenide WS_2 Films Prepared with a Combination of Spin/Dip Coating and CVD

Woon-Seop Choi*

Department of Semiconductor Engineering, Hoseo University, Asan, Chungnam 31499, Republic of Korea

Abstract: Recently, transition metal dichalcogenides (TMDCs) with 2D structure have attracted interest due to their many unique optical and electrical properties. The primary preparation methods for 2D materials are chemical vapor deposition (CVD), exfoliation, and other vacuum technologies. Large-scale synthesis of WS_2 via solution-process is rare due to the higher temperature needed for tungsten-based precursors. Combination of spin coating or dip coating with CVD have been studied recently to make large-area 2D TMDC with good electrical properties. Here, we report a new synthetic route for large WS_2 crystal that combined solution coatings and CVD process. A solution of sodium tungstate and hydrazine hydrate with sodium thiosulphate was coated on a silicon wafer via dip and spin coating. The films were then treated with CVD at various positions and temperatures to facilitate crystallization. The double coating conditions and CVD parameters were modified to obtain WS_2 crystals. Triangular shaped 44 ± 4 μm WS_2 crystals could be obtained with simple annealing above 900°C without gas treatment. The synthesized WS_2 was found to be bulk with a triangular shape, as confirmed by Raman and AFM analyses. A PL peak of WS_2 at 643 nm was observed at an early crystallization stage.

(Received 4 May, 2023; Accepted 27 June, 2023)

Keywords: 2D, TMDC, WS_2, CVD, solution process

1. INTRODUCTION

Even though graphene has many potential uses, including electrical, optical, and biomedical applications, the practical realization of graphene seems limited by its band gap of zero. Recently, in the field of nanoelectronics and optoelectronics, two-dimensional (2D) transition metal dichalcogenides (TMDC), which are analogous to graphene, have attracted considerable attention because of their electrical and innate band gap characteristics. These can be divided into semiconductor, semimetal, and metal characteristics because of the coordination of TMDCs.

Among them, MoS_2 and WS_2 show particular interesting properties. They have a direct and indirect band gap of 1.8 eV and 1.2 eV, respectively, depending on the monolayer stacking states. Thin layered WS_2 composed of a S-W-S crystalline sandwich with a van der Waals bonding, possess the coupled spin and valley physics [1], and high photoluminescence efficiency [2]. It can also be used in composited layered materials with other 2D materials for many applications [3]. Most studies on 2D TMDC have been focused on their chemical synthesis using chemical vapor deposition (CVD), and by mechanical methods like exfoliating flakes by tape or in liquid.

In order to make large-area and high-quality 2D TMDC with good electrical properties, various spin coating or dip coating methods combined with CVD methods have been intensively studied in the last few years. High thermal annealing of thermally decomposed ammonium thiomolybdate with sulfur resulted in highly crystalline MoS_2 after dip coating [4]. A bottom gate transistor with synthesized MoS_2 was demonstrated and showed electron mobility comparable to that of micromechanically exfoliated MoS_2 nano-sheets. The highly controllable thickness of MoS_2 thin film grown via a spin-coating route resulted in wafer-scale homogeneity with crystalline and stoichiometric chemical composition [5]. Our group reported a new solution synthesis route for MoS_2 films

- 최운섭: 교수
*Corresponding Author: Woon-Seop Choi
[Tel: +82-41-540-5924, E-mail: wschoi@hoseo.edu]
Copyright ⓒ The Korean Institute of Metals and Materials

with one step annealing without CVD for the first time [6]. New electrohydrodynamic jet patterned MoS_2 films were reported from precursor solution with one step annealing [7]. More recently, deionized (DI) water-based solution processed MoS_2 was also reported [8].

However, the CVD method for WS_2 crystal layers is more challenging than MoS_2 because of the higher temperature needed for tungsten-based precursors. In some case, WS_2 bulk powder can be formed by the direct reaction of sulfur with the bulk WO_3, which stops the growth of the domains of WS_2. Therefore, two furnace systems were used in CVD to accurately control the time for introducing sulfur to make large WS_2 domains [9]. It is not possible to obtain large WS_2 from mechanical exfoliation due to the difficulty in taking a crystalline layer from a clump.

WS_2 was also obtained by the evaporation of WO_3 by hydrogenation and sulfurization in CVD with H_2 and Ar under low pressure [10]. Controlling H_2 concentration was crucial to obtain large crystals. Using ambient pressure during the CVD, large single-crystal WS_2 was prepared on Au foil by a surface growth mechanism. It could be transferred to any substrates, without wrinkles or damage by using an electrochemical bubbling technique. However, an expensive Au substrate was used because it does not react with sulfur, and acts as a catalyst to lower the reaction energy [11].

Large-scale synthesis of WS_2 via solution-process is rare. WS_2 nanosheets with a lateral dimension of 100 nm were prepared from 1D $W_{18}O_{49}$ with surfactants and a rolling-out method, A powder of WS_2 nano-sheet was prepared by a two-step method of ball-milling and thermal annealing. A hydrothermal reaction was employed to obtain a 2D nano-sheet, but it was not easy to obtain a 2D form because WOx prefers 1D or 0D formation, in contrast to MoS_2 [12]. Recently, the facile fabrication of WS_2 was demonstrated using a thermal decomposition of precursor with two annealing processes. The first annealing step was used to achieve the lateral epitaxial growth of the WS_2 and the second annealing was in S-rich and high-temperature conditions [13]. Atomically thin WS_2 from a solution process was reported using CVD under H_2 gas, and it was applied to optoelectronic devices [14]

We have prepared a new synthesis route by combining solution coating and a CVD process. In order to obtain a uniform and large size WS_2 crystal, a solution of sodium tungstate and hydrazine hydrate with sodium thiosulphate was coated on a silicon wafer with controlled parameters via two coating methods; dip coating and spin coating. The coated wafer was thermally treated with CVD using sulfur with different positions and temperatures to investigate the crystalline formation. Large-scale WS_2 crystals with triangular shape could be obtained.

2. EXPERIMENTAL

The precursor solution was prepared as follows, 5 mL of (0.25 M) sodium tungstate in hydrazine hydrate, 2.5 mL of (0.1 M) citric acid, and 10 mL of (0.25 M) sodium thiosulphate were added to 50 mL of DI water. P-type Si wafer with a thermally-grown 300 nm layer of SiO_2 was cleaned with IPA, acetone and DI water. The wafer was treated with UV/O_3 for 10 min to improve surface wettability and obtained better film coverage. After the precursor solution was heated to 70°C in an oil bath, the silicon wafer substrate was dipped into the precursor solution for 1h 30 min to coat it. After it was removed from the solution, the substrate was spin-coated with the precursor solution at 2000 rpm for 30 s.

After soft baking the substrate at 150°C for 15 min, the sample was treated by CVD with sulfur powder and annealed for 30 min under N_2 flow at various positions at temperatures of 600°C to 1000°C. The sample positions were 25 cm, 35 cm, and 40 cm from the inlet, and the sulfur was positioned at 5 cm from the inlet. The temperature and relative humility were controlled to keep the evaporation conditions stable during the experiment. Raman spectra and PL were collected with a confocal Raman spectrometer (LabRAM HR800) using a 532-nm laser as an excitation source. The laser spot size was approximately 1 μm at 60 μW.

3. RESULTS AND DISCUSSION

To prepare a suitable solution for the WS_2 precursor, several compounds were tested, and sodium tungstate was chosen. A solution formulation was developed with a mixture of hydrazine and sodium thiosulfate in DI water. However, solid film could not be formed on the substrate by dip coating

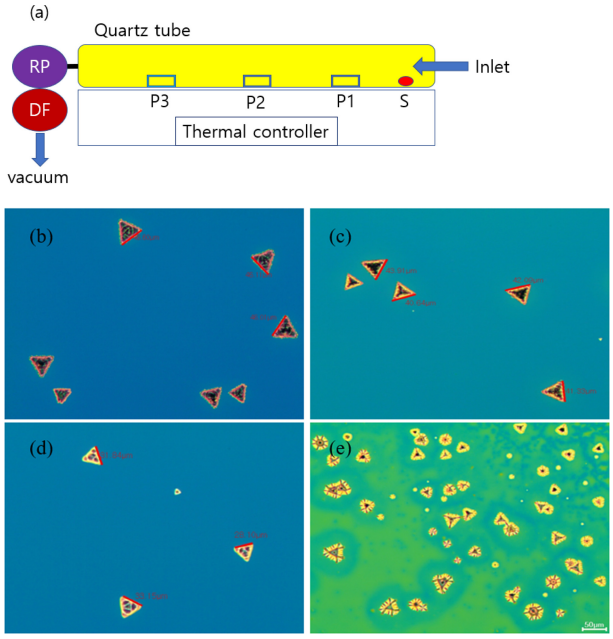

Fig. 1. (a) Distance of the samples from the inlet in CVD, P1; 25 cm, P2; 35 cm, P3; 40 cm, and S; sulfur (rotary ,RP, and diffusion, DF, pump systems). (b-e) OM images of WS_2 at (b) 1000, (c) 900, (d) 800, and (e) 600°C of annealing temperatures

with the solution formulation. With spin coating, the precursor film was not uniformly formed even after surface treatment of the substrate with UV/O_3. The combination of dip and spin coating was employed to obtain better films. To create some seed layers, an initial dip coating was performed. Spin-coating could then be performed on the seeded layer to obtain uniformly coated films. These two coating steps provided solid films on wafer.

Thermal treatment is then required to promote crystal growth from the wet precursor films. To make WS_2 crystals, the double-coated layer was inserted into a reactive furnace with sulfur powder, as shown in Fig. 1. The effect of furnace temperature on the crystal growth was investigated. Interestingly, the formation of WS_2 films started from 600°C. Perfect crystals were formed at 900°C and 1000°C, but, the crystals also started growing at much lower temperatures, as shown in Fig. 1b-e. When annealed, the chamber was maintained at a low pressure of 35 Torr with a nitrogen flow of 5.2 sccm for 30 min for inert conditions.

The amount of sulfur was another factor to control. Sulfur was placed at 5, 8, and 11 cm from the inlet of the furnace. When the sulfur was placed at a distance of 5 cm, the WS_2 crystals had a normal shape with broad distribution. However, when the distance was increased to 8 and 11 cm, the WS_2 crystal shape was changed, and relatively uneven crystals were observed. Therefore, the distance was fixed at 5 cm with different annealing temperatures (600, 700, 800, 900, and 1,000°C).

The sample position was varied to 25, 30, and 40 cm from the furnace inlet, as shown in Fig 1a. The size distribution of WS_2 varied with not only sulfur position, but also sample positions. The average size was around 44 ± 4 μm for a position 25 cm from the inlet. It was around 40 ± 5 μm for 30 cm and around 32 ± 6 μm for 40 cm position, as shown in Fig. 1b. It is not easy to draw conclusions about the dependence of sample position and crystal size. The farthest position from the inlet, 40 cm, showed a relatively broad distribution of crystal, and random shapes of crystals were observed. In general, a position closer to the inlet led to relatively large crystal size and even size distributions. This was because the sulfur powder was more easily accessible, which it was closer to the precursor-coated sample.

When the temperature was lower than 900°C, crystal growth was different, depending on the sample position. For example, at 800°C, the crystal growth was incompletely finished due to the low annealing temperature. At 30 cm and 40 cm, triangle-shaped crystals of WS_2 were observed with star-shape and rectangular crystals. These incomplete crystal growths were due to the annealing temperature, which was not high enough, and the lower availability of sulfur powder due to the long traveling distance. When the annealing temperature was 600°C, a few crystalized triangular crystals were observed, but there were many under-crystalized domains, like islands on the sea, as shown in Fig. 1e. When the annealing temperature was over 900°C, all WS_2 were crystalized into triangular shapes, regardless of the positions. The triangular shaped WS_2 with multi apex is attributed to the growth rate of the W and S.

The effect of annealing temperature can be clearly understood from the OM images of WS_2 crystals with temperatures, as shown in Fig. 1b-e. In general, a higher thermolysis temperature leads to higher crystallinity in the WS_2 film. At 900 and 1000°C, WS_2 crystals were obtained with a relatively large size and even distribution. A WS_2 crystal size of around 44 μm was obtained at the annealing

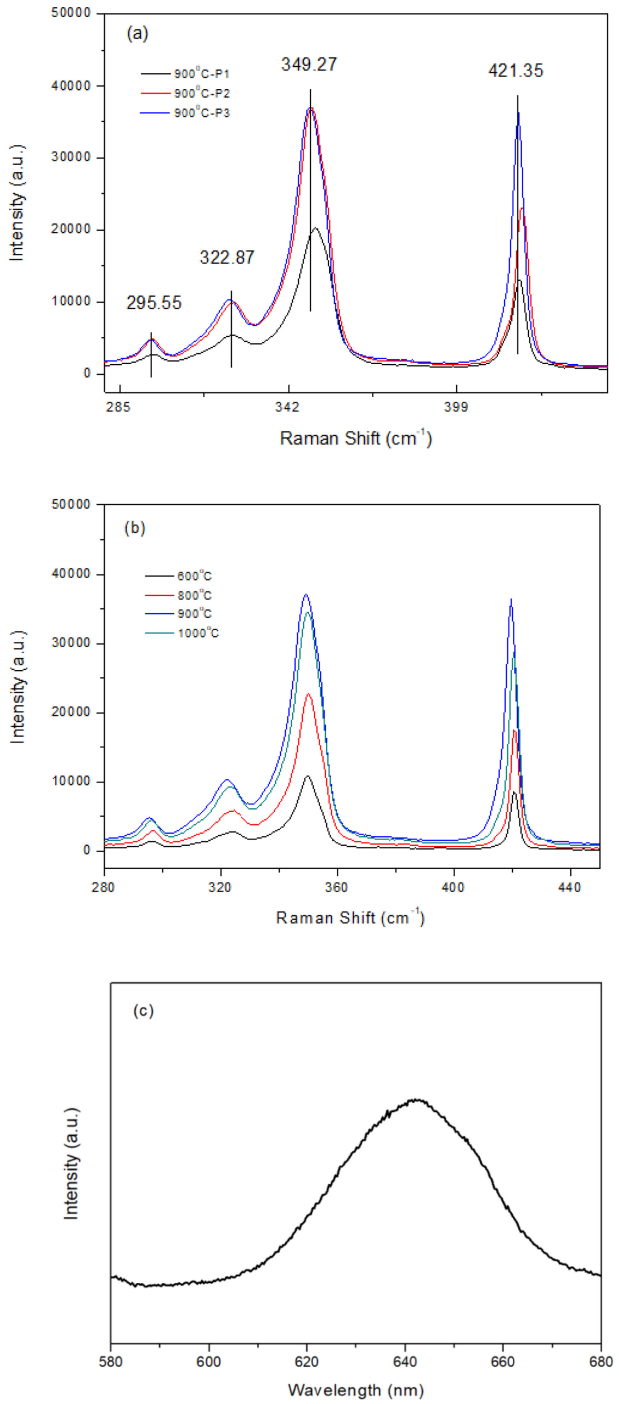

Fig. 2. (a) Raman spectra of synthesized WS_2 with different sample positions in CVD, (b) Raman spectra of WS_2 at various annealing temperatures. (c) PL spectrum of synthesized WS_2 showed at 643 nm.

temperature of 1000ºC. However, at 800ºC, the crystal size was reduced because there was insufficient crystallization. Premature crystal shapes were observed at 600ºC.

We confirmed that relatively large size 42 - 48 μm of WS_2 crystal could be obtained with the double coating. In the literature, when two furnaces in separate systems were used to control the sulfur, mostly small sizes of WS_2 were reported [9]. With another CVD method with WO_3, no WS_2 could be formed without H_2 gas, and WS_2 crystals were observed under H_2/Ar gas mixture [10]. However, we obtained large WS_2 crystals through simple annealing without H_2 gas.

Raman spectra can be used to characterize the synthesized WS_2 films, as shown in Fig. 2. The in-plane optical mode of E^1_{2g} for WS_2 appears at approximately 350 cm^{-1}. The out-of-plane vibration of sulfur of A_{1g} appears at 421 cm^{-1}. As seen in Fig. 2a, the different sample positions in the furnace affects the peak intensity of the Raman spectra. A similar effect on crystal sizes was mentioned above. The closest position, P1 (25 cm from inlet of furnace), showed the highest peak among the positions. Compared with another WS_2 synthesis method, Raman peaks showed E^1_{2g} at 355-358 cm^{-1} and A_{1g} at 417-419 cm^{-1} depending on the synthesis methods. The double coating methods shows a lower E^1_{2g} and higher A_{1g}, and a larger a difference for different positions.

In general, the position of these two peaks and their difference provide information on the number of layers in the crystals. When the frequency difference is around 60 to 64 cm^{-1}, WS_2 will have 1 to 5 layers. Above this, the samples are classified as bulk materials. Therefore, from the difference in the two peaks at 71 cm^{-1}, the films from our solution method can be considered bulk.

It is hard to identify these multi-phonon bands in the two other peaks of WS_2 that appear at 295 and 322 cm^{-1} (Fig. 2a), which may be assigned as the combination modes of 2LA-$2E^2_{2g}$, and 2LA-E^2_{2g} [13] or 2ZA(M) and LA(M)+TA(M) [15]. Charting th Raman spectra with annealing temperatures to show the intensity of the peaks with temperatures, the higher peaks appear with higher temperatures. The same trend and peaks can be observed at the lowest temperature of 600ºC. Interestingly, the Raman peaks for sample temperature above 900ºC show that the sample closest to the inlet had the highest peak intensity, which can also be confirmed from Fig 2b.

The triangular crystals and the thickness are clearly demonstrated in AFM measurements, as shown in Fig. 3. The AFM image shows an approximately 125-nm thickness with

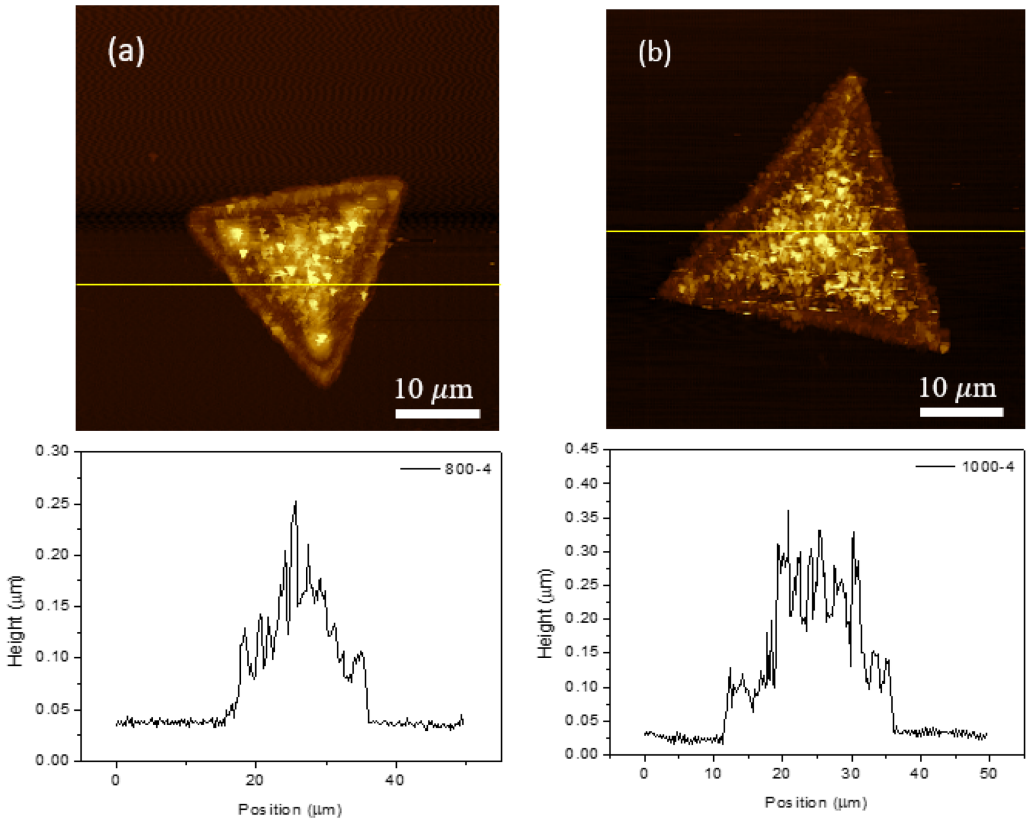

Fig. 3. AFM images and thickness profiles of WS_2 at annealing temperature of 800 and 1000°C.

3.2-nm roughness at 800°C and 200-nm thickness with 6.2-nm roughness at 1000°C. The WS_2 films are relatively thick layers, which may be the result of the double coating methods. A relatively thick layer is formed due to the dip coating to make a seed layer on the substrate. We found that it was not possible to make a film by simple spin coating only. Dip coating is also critical for film formation, and seed molecules from the dip coating keep the precursor solution on the substrate during spin coating and increase nucleation density.

Even though a spin coating technology is available using diluted $(NH_4)_2WS_4$ solution, H_2 gas is needed to protect the effect of oxygen on the crystallization of WS_2 films during annealing [13, 14]. WS_2 has also been obtained by the reduction and sulfurization of WO_3 with high H_2 concentration [10]. Even though mono- to multi-layers of WS_2 could not be obtained, unlike other studies no gas was used during our process. And we obtained relatively large sized triangular WS_2 crystals on wafer, which are suitable for potential applications.

The WS_2 monolayer showed strong PL emission with strong spin-orbital coupling. The PL peaks for mono- and bilayers were reported to be 641 nm with a sharp and narrow FWHM [10]. In general, PL peaks are rarely observed in multi-layer WS_2 because of the change from a direct to an indirect band gap [16]. The triangular shaped WS_2 showed a broad PL spectrum at 643 nm at 700°C, as shown in Fig. 2c. The reason might be that mono- or few-layer WS_2 could have formed during an early stage of crystallization annealing. After crystallization, no peak was observed due to the multi or bulk crystals.

4. CONCLUSIONS

To obtain large WS_2 crystals from solution synthesis, a combined dip and spin coating method with CVD was developed. The effect of sample position and sulfur during CVD was investigated with a focus on the crystal size and

distribution of WS_2. The sample position of 25 cm from the CVD inlet and 5 cm from the sulfur source were suitable to obtain triangular crystals. Even though the annealing temperature is crucial for crystallization, WS_2 starts to form crystal at the relatively low temperature of 600ºC, with complete crystallization above 900ºC. The relatively large size of around 44 ± 4 μm WS_2 could be obtained from the solution method by simple annealing without gas treatment. The resulting WS_2 was found to be a bulk material using the double coating method, as confirmed by Raman and AFM. Interestingly, a broad PL peak was obtained from the WS_2 film prepared at 700ºC. This might be the early stage of crystal formation before growing into bulk material. Further work is necessary to control the atomic layers of WS_2 for optoelectronic applications.

ACKNOWLEDGEMENT

This work was supported by the Basic Science Research Program through the National Research Foundation Korea (NRF-2018R1D1A1B07048441) and Regional Innovation Strategy (RIS) through the NRF funded by the Ministry of Education (MOE, 2021RIS-004).

Competing interests

The authors declare no competing interests.

REFERENCES

1. H. Zeng, G.-B. Liu, J. Dai, Y. Yan, B. Zhu, R. He, L. Xie, and X. Chen, *W. Yao, Sci. Rep.* **3**, 1608 (2013).
2. W. Zhao, Z. Ghorannevis, L. Chu, M. Toh, C. Kloc, P. Tan, and G. Eda, *ACS Nano.* **7**, 791 (2013).
3. K. Kosmider, J. Fernandez-Rossier, *Phys. Rev. B.* **87**, 075451 (2013).
4. K.-K. Liu, W. Zhang, Y.-H. Lee, Y.-C. Lin, M.-T. Chang, C.-Y. Su, C.-S. Chang, H. Li, Y. Shi, H. Zhang, C.-S. Lai, and L.-J. Li, *Nano Lett.* **12**, 1538 (2012).
5. J. Yang, Y. Gu, E. Lee, H. Lee, S. H. Park, M.-H. Cho, Y. H. Kim, Y.-H. Kim. And H. Kim, *Nanoscale* **7**, 9311 (2015).
6. Y. J. Kwack and W.-S. Choi, *Nanotechnology* **30**, 385201 (2019).
7. T. T. T. Can and W.-S. Choi, *Mater Design* **199**, 109408 (2021).
8. Kwack, T. T. T. Can and W.-S. Choi, *npj 2D Mater Appl* **5**, 84 (2021).
9. Y Rong, Y. Fan, A. L. Koh, A. W. Robertson, K. He, S. Wang, H. Tan, R. Sinclair, and J. H. Warner, *Nanoscale* **6**, 12096 (2014).
10. K. N. Kang, K. Godin, and E.-H. Yang, *Sci Rep.* **5**, 13205 (2015).
11. Y Gao, Y. Gao, Z. Liu, D.-M. Sun, L. Huang, L.-P. Ma, L.-C. Yin, T. Ma, Z. Zhang, X.-L. Ma, L. M. Peng, H.-M. Cheng, and W. Ren, *Nat. Comm.* **6**, 8569 (2015).
12. J Yang, D. Voiry, S. J. Ahn, D. Kang, A. Y. Kim, M. Chhowalla, and H. S. Shin, *Angew. Chem. Int. Ed.* **52**, 13751 (2013).
13. Z. Li, S. Jiang, S. Xu, C. Zhang, H. Qui, P. Chen, S. Gao, B. Man, C. Yang, and M. Liu, *J. alloys Compd* **666**, 412 (2016).
14. K. C. Kwon, C. Kim, Q. V. Le, S. Gim, J. M. Jeon, J. Y. Ham, J. L. Lee, H. W. Jang, and S. Y. Kim, *ACS Nano* **9**, 4146 (2015).
15. W. Zhao, Z. Ghorannevis, K. K. Amara, J.R. Pang, M. Toh, X. Zhang, C. Kloc, P. H. Tane, and G. Eda, *Nanoscale* **5**, 9677 (2013).
16. W. Zhao, R. M. Ribeiro, M. Toh, A. Carvalho, C. Kloc, A. H. C. Neto, and G. Eda, *Nano Lett.* **13**, 5627 (2013).